Multiplexed EFPI sensors with ultra-high resolution

Nikolai Ushakov*, Leonid Liokumovich
Department of Radiophysics, St. Petersburg State Polytechnical University

ABSTRACT

An investigation of performance of multiplexed displacement sensors based on extrinsic Fabry-Perot interferometers has been carried out. We have considered serial and parallel configurations and analyzed the issues and advantages of the both. We have also extended the previously developed baseline demodulation algorithm for the case of a system of multiplexed sensors. Serial and parallel multiplexing schemes have been experimentally implemented with 3 and 4 sensing elements, respectively. For both configurations the achieved baseline standard deviations were between 30 and 200 pm, which is, to the best of our knowledge, more than an order less than any other multiplexed EFPI resolution ever reported.

Keywords: fiber-optic sensors, multiplexing, signal processing, extrinsic Fabry-Perot interferometer, spectral measurements, phase measurements, interference.

1. INTRODUCTION

During the last two decades a great progress in manufacture and implementation of the fiber optic sensors based on the extrinsic Fabry-Perot interferometers (EFPI)[1] has been achieved by the academic institutions and commercial companies. Such sensors demonstrate a great dynamic measurement range and a high resolution[2,3]. Sensors of a great variety of physical quantities have been designed and implemented. The most commonly used EFPI baseline demodulation approaches are two white-light interferometry methods[4]: using of a scanning readout interferometer and measuring the spectral function of the tested interferometer. Both these techniques provide an ability to obtain the absolute baseline value and to track the signals of a system of multiplexed interferometers with different baseline values[5,6]. However, according to the recent progress in the field, the spectrum measurement approach is more advantageous, with the best baseline resolution of a single sensor about 10 picometers[2,3], whereas for the multiplexed sensors the best achieved resolution was about 1 nanometer[5]. Therefore, the spectrum measurement approach is considered exclusively within the current paper. Despite the experimental progress in the field, the theory of such sensors isn't well developed and, to the best of our knowledge, no analytical description of their possible performance is presented in literature. So, the scope of the current work is to introduce some fundamentals of such description and to achieve the baseline resolution comparable with the one attained for the single-sensor devices.

Throughout this paper we consider the case of registering the spectrum of the light reflected from the sensor, which is the most common case for both single-sensor and multiplexed systems. The spectral function of a low-finesse Fabry-Perot interferometer is quasi-harmonic, and is expressed as $S_{FP}(L, \lambda) = S_0(L, \lambda) + S_M \cdot S(L, \lambda)$, for the reflected light:

$$S(L, \lambda) = \cos[4\pi nL/\lambda + \gamma_R(L, \lambda)], \quad (1)$$

$$S_M = (R_1R_2)^{1/2} w/w(L) \approx (R_1R_2)^{1/2} \pi n w^2/2\lambda L_e, \quad (2)$$

where $\gamma_R(L, \lambda) = -\arctan(2L\lambda/\pi n w^2) + \varphi_R$; $w(L)=[w^2+(L\lambda)^2/(\pi n w)]^{1/2}$; L is the interferometer baseline; λ is the light wavelength; n is the refractive index of the media between the mirrors; the first term in $\gamma_R(L, \lambda)$ is a Gouy phase shift[7], an additional phase term φ_R is induced by the mirrors (typically for dielectric mirrors $\varphi_R=\pi$); w is an effective radius of a Gaussian beam at the output of the first fiber, which is close to the fiber mode field radius. These equations are valid for the case of parallel mirrors and relatively large L. Transfer function of a system of N multiplexed EFPIs with different baselines L_k, k=1..N is a superposition of quasi-harmonic signals (1) with different frequencies and can therefore be expressed as

$$S_{MULT}(L_1,\ldots,L_N,\lambda) = \sum_k S'_{Mk} S_k(\lambda) + H(L_1,\ldots,L_N,\lambda), \quad (3)$$

where $S_k(\lambda)=S(L_k, \lambda)$; S'_{Mk} amplitudes are discussed in detail in the next section; $H(L_1,\ldots L_N, \lambda)$ contains quasi-static component and a number of parasitic components, with baselines different from $L_1,\ldots,L_N$ and must be filtered out. Therefore, extracting partial spectra $S_k(\lambda)$ and applying the baseline demodulation approaches developed for a single sensor, one can obtain the readings from each multiplexed sensor.

* Corresponding author: n.ushakoff@spbstu.ru

2. SENSORS PERFORMANCE ANALYSIS

The amplitude S'_{Mk} is one of the main parameters, defining the possible resolution of the k-th sensor, therefore, one of the main aims of this section is to introduce the estimations for S'_{Mk}. Also the problem of cross-talk in multiplexed interferometric sensors is quite important, though, for EFPI it is often neglected[5]. However, for ultra-high resolution sensors its sources must properly be taken into account in order to ensure the absence of any evidence of it.

In parallel configuration (see figure 1, (a) for example) the light intensity brought to each interferometer is determined by the division ratios at the coupling elements. For the most obvious case of uniform power distribution between the sensors, the corresponding amplitudes S'_{Mk} can be expressed as

$$S'_{Mk}=1/N^2(R_{1k}R_{2k})^{1/2}(\pi n w^2)/(2\lambda_0 L_k). \quad (4)$$

In order to minimize the variance of S'_{Mk} amplitudes, a nonuniform distribution of the light power over the sensors can be used, in this case the estimate (4) must be modified. The lengths of the feeding fibers must be chosen sufficiently different in order to suppress parasitic interference signals, therefore, component $H(\lambda)$ in (3) will be stipulated only by the higher harmonics of the Airy function ((1) contains only the first harmonic of the Airy function).

In serial scheme (see figure 1, (b) for example) the interferometers are connected to the sensor interrogator one after another, therefore, considering the signal of the k-th interferometer, one must take into account the light propagation through the preceding interferometers. Spectrum of the light, reflected from the k-th EFPI, can be written as $[S_{T1}(\lambda)\cdot\ldots\cdot S_{Tk-1}(\lambda)]^2\cdot S_k(\lambda)$, the EFPI spectral function for the transmitted light $S_{Tj}(\lambda)$ is written below

$$S_{Tj}\left(L_j,\lambda\right)=S_0\left(L,\lambda\right)+S_{MT}\cdot S_T\left(L_j,\lambda\right)\cong\left(1-R_1\right)\left(1-R_2\right)\frac{w^2}{w^2\left(L_j\right)}\left\{1+2\sqrt{R_1R_2}\,\frac{w\left(L_j\right)}{w\left(3L_j\right)}\cos\left[4\pi nL_j/\lambda+\gamma_T\left(L_j,\lambda\right)\right]\right\}, \quad (5)$$

where $\gamma_T(L,\ \lambda) = \arctan(L\lambda/\pi n w^2) - \arctan(3L\lambda/\pi n w^2) + \varphi_T$, φ_T is induced by the mirrors' reflections, typically for dielectric mirrors $\varphi_T=0$; as for (1) and (2), an assumption of parallel mirrors was used. The static summand in (5) is constant and determines the mean transmitted optical power. Therefore, the expression for S'_{Mk} can be written in the following form

$$S'_{Mk}\approx\frac{\sqrt{R_{1k}R_{2k}}\cdot\left(\pi n w^2/\lambda_0\right)^{4k-3}}{2L_k}\cdot\prod_{j=1}^{k-1}\frac{\left(1-R_{1j}\right)^2\left(1-R_{2j}\right)^2}{L_j^4}, \quad (6)$$

where λ_0 is the central wavelength. Herein an assumption of Gaussian profile of the free-space (inside the interferometer) and fiber modes was made, allowing to approximate the power coupled from the free-space beam to the fiber mode as proportional to squared modes radii. According to our experimental results, these assumptions are valid in (2) for the case L>200μm and in (5) and (6) for the case L>400μm. However, in practical case one might utilize sensors with smaller L values (see section 3 for examples); in this case the values S'_{Mk} calculated according to (6) will be underestimated.

The oscillating summand in (5) doesn't affect the mean optical power and will modulate the light spectrum brought to the k-th sensor, resulting in the uprising of parasitic components of the form $a\cdot S_k(\lambda)\cdot S_T(L_j, \lambda)$, $j<k$ in S_{MULT}. In such a manner, overall spectrum S_{MULT} will contain parasitic components corresponding to baselines combinations $L_k \pm L_j$.

Therefore, the main origin of the cross-talk in the considered systems is coincidence of the oscillation periods of the parasitic $H(\lambda)$ and the target $S_k(\lambda)$ components in (3) the optical paths differences (OPDs) in different EFPIs. In order to avoid the cross-talk, the following condition on the cavity lengths must be fulfilled $|L_k - (p\cdot L_i + q\cdot L_j)| >> \Delta L$, where p,q are integer, the worst cases are p=2, q=0 or p=±1, q=±1, $|i-j|$=1; $\Delta L = \lambda_0^2/2n\Lambda$ is the resolution in the interferometer baseline domain after applying Fourier transform to $S(\lambda)$ function. Considering a sum of target and parasitic quasi-harmonic signals of form (1) with close frequencies and significantly different amplitudes A and a, we obtain $A\cdot S(L_1, \lambda) - a\cdot S(L_2, \lambda) \approx A\cdot\cos[4\pi n(L_1 + a/A\cdot(L_1 - L_2))/\lambda + \gamma]$, with the resultant error given by

$$\delta L = a/A\cdot(L_1 - L_2). \quad (7)$$

Values of A and a can be analyzed separately, which is out of the scope of the current paper, however, for a practical case a/A about 0.01 (see figure 3 for example) and δL about 100 nm the resulting deviation of the registered baseline from the real one will be about 1 nm, which is around an order greater than the achievable displacement resolutions (see table 1 below).

3. EXPERIMENTAL DEMONSTRATION

Both parallel and serial multiplexing schemes were realized experimentally, the experimental setups are shown in figure 1 (a) and (b), respectively. The parameters of the optical setups were the following: in parallel scheme L_1=41μm, L_2=195μm, L_3=526μm, L_4=719μm; in serial scheme L_1=42μm, L_2=170μm (one fiber end was evaporated), L_3=250μm (Si plate); the resulting reflectivities are shown in figure 1. The optical power at the interrogator output was 100 μW. The spectra acquisition rate was about 1 Hz.

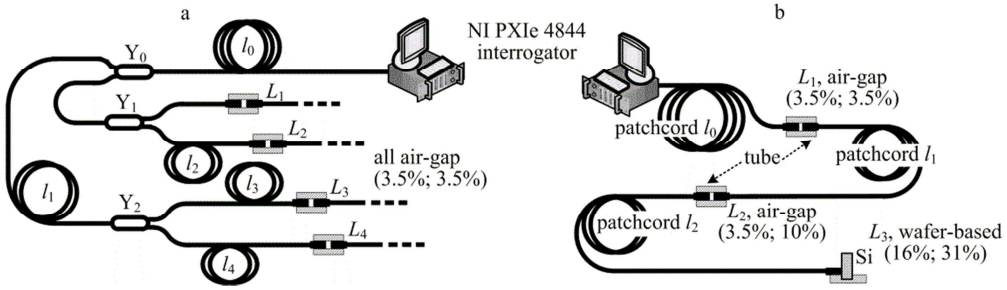

Figure 1. Experimental setups for serial (a) and parallel (b) configurations.

Signal processing was running on a PXI chassis controller. In order to simplify the processing, we assumed that the baselines are known with accuracy ~30 μm. Therefore, the partial element spectra $S_k(\lambda)$ could be extracted by pre-defined band-pass filters, which was done by the same way as in[6]. After that, for each $S_k(\lambda)$ spectrum the approximation-based approach described in[2] was applied. The standard deviations of the estimated baselines σ_{Lr}, shown in table 1, were calculated over the temporal intervals about 10 minutes, corresponding to 600 baseline samples for each sensor.

Table 1. Standard deviations of the baseline measurements for serial and parallel multiplexing configurations.

	L_1, parallel	L_2, parallel	L_3, parallel	L_4, parallel	L_1, serial	L_2, serial	L_3, serial
σ_{Lr}, pm	41	63	180	200	32	43	78

In figure 2 the FFTs of the registered spectra of parallel (a) and serial (b) schemes are shown, *x* axis corresponds to the air-gap cavity length. For the Si-plate sensor it should be properly recalculated with taking into account Si refractive index with dispersion. It is clearly seen in figure 3 (b) that in the spectral function of serially multiplexed EFPIs, components corresponding to OPDs combinations are presented along with single, double and triple OPDs.

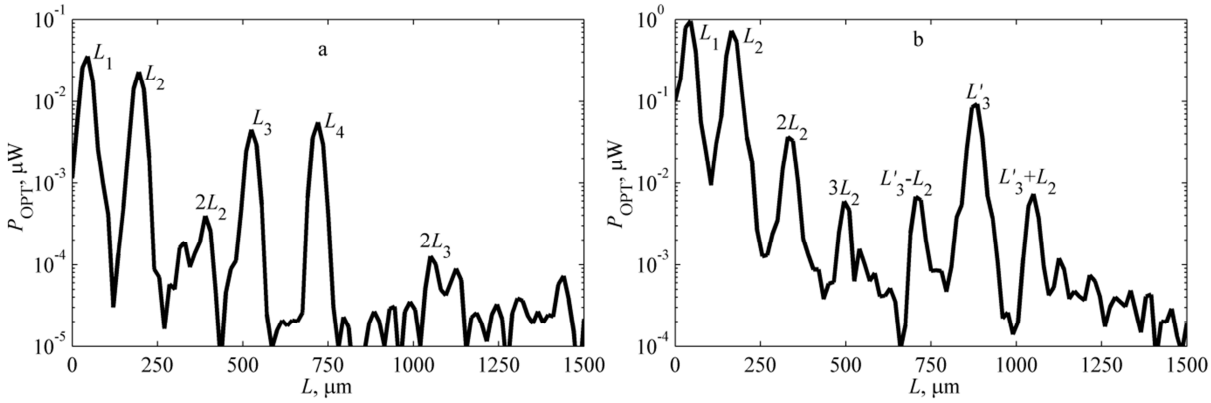

Figure 2. FFTs of the multiplexed EFPIs spectral functions.

For the parallel configuration S'_{Mk} amplitudes calculated according to (4) are in a good accordance with the experimentally observed values (figure 2, (a)), except the first sensor (L_1=41μm), for which the above assumptions are not valid. For the serial configuration S'_{Mk} estimations for the 2-nd and the 3-rd sensors made according to (6) are about an order less than the experimental values due to the approximations in (5) and (6), which are not fulfilled for the first sensor with its baseline L_1=42μm.

In order to study the sensing abilities of the assembled systems and ensure the absence of the cross-talk, we have consequently heated and cooled one of the sensors, while the rest were placed into the thermally isolated chamber. This operation was repeated for both configurations and all combinations of heated/isolated sensors. In figure 3 the corresponding baseline curves are illustrated. In figure 3 (a) the heating of the 4-th sensor in parallel scheme is

illustrated, in figure 3(b) – the heating of the first sensor in serial scheme. Curves of the deviations of non-perturbed sensors baselines demonstrate no correlation with the perturbed, hence, no cross-talk was present in the current systems, at least, at the levels limited by the sensors resolutions. The range of the temperature changes was 13-15 K, from this the baseline temperature sensitivity of air-gap sensors can be estimated about 6.4 nm/K.

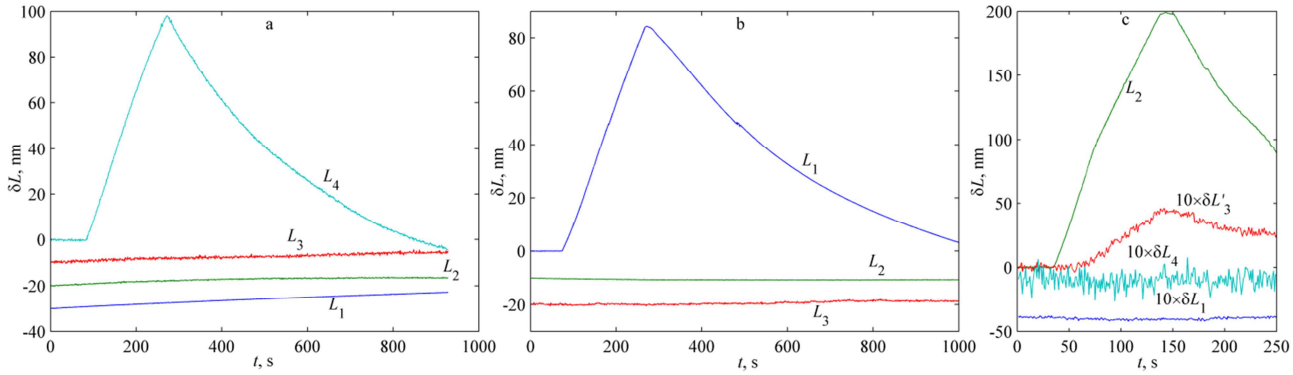

Figure 3. Experimental results of single-sensor heating.

In a separate experiment with parallel setup L_3 was changed to ~390 μm to match the doubled L_2. In such a manner, by heating the 2-nd sensor the cross-talk effect (δL_2 influencing the 3-rd sensor readings) was demonstrated. The initial values and additional shifts were subtracted from the curves for better demonstrativeness. For the same reason the curves of L_1, L_3 and L_4 variations in figure 3 (c) were 10 times magnified. The parasitic deviation of L_3 shown in figure 3 (c) is in accordance with expression (7).

4. CONCLUSION

A brief analytical analysis of the multiplexed EFPI sensors of serial and parallel configurations has been carried out. We have considered the effects, determining the resolution of such sensors and the possible cross-talk. An experimental realization of the both considered configurations was made, for the both the baseline standard deviations between 30 and 200 pm were achieved. As can be predicted from (4), setting R_{2k}≈100%, one can attain nearly the same signals strengths for the parallel scheme with 8 elements, as in the performed experiment, and hence, nearly the same baseline resolutions.

REFERENCES

[1] Fang, Z., Chin, K. K., Qu, R. and Cai, H., [Fundamentals of Optical Fiber Sensors], Wiley, New Jersey, 395-426, (2012).

[2] Ushakov, N., Liokumovich, L. and Medvedev, A., "EFPI signal processing method providing picometer-level resolution in cavity length measurement," Proc. SPIE 8789, 87890Y (2013).

[3] Wang, W. and Li, F., "Large-range liquid level sensor based on an optical fibre extrinsic Fabry–Perot interferometer," Opt. Lasers Eng., 52, 201-205 (2014).

[4] Jiang, Y. and Ding, W., "Recent Developments in Fiber Optic Spectral White-Light Interferometry," Phot. Sens. 1 (1), 62-71 (2011).

[5] Wang, J., Dong, B., Lally, E., Gong, J., Han, M. and Wang, A. "Multiplexed high temperature sensing with sapphire fiber air gap-based extrinsic Fabry-Perot interferometers," Opt. Lett. 35(5), 619-621 (2010).

[6] Jiang, Y. and Tang, C., "Fourier transform white-light interferometry based spatial frequency-division multiplexing of extrinsic Fabry-Perot interferometric sensors," Rev. Sci. Instrum. 79 (10), 106105 (2008).

[7] Banerjee, P. P. and Poon, T.-Ch., [Principles of Applied Optics], Aksen Associates, Inc., Boston, 50-120, (1991).